



## PERFORMANCE ASSESSMENT OF A LOW-COST SEISMIC ISOLATION PROTOTYPE USING RECYCLED RUBBER

R. Reyna<sup>(1)</sup>, A. Muñoz<sup>(2)</sup>, C. Zavala<sup>(3)</sup>

<sup>(1)</sup> Associate Professor, National University of Engineering, rreynas@uni.edu.pe

<sup>(2)</sup> Research Assistant, Japan-Peru Center for Earthquake Engineering Research and Disaster Mitigation, amunozf@uni.pe

<sup>(3)</sup> Professor, National University of Engineering, czavala@uni.edu.pe

### **Abstract**

According to the philosophy of seismic design of buildings of the Peruvian Earthquake Resistant Standard, buildings must be design to keep the life of the inhabitants safe. The seismic design of essential buildings such as health centers, as well as buildings that could be used as shelters in case of disaster, must ensure that those buildings remain operational and functional post disaster. For this reason, it is necessary to protect seismically the structure. To do so, many technologies have been developed and implemented throughout the world, one of them is the seismic isolation system of structures. Peruvian standard requires that certain health center buildings must use a seismic isolation system to seismically protect the building. However, common buildings such as dwellings, are not required to use seismic protection of buildings. Due to the high cost of seismic isolation systems, a prototype of low-cost seismic isolation using recycled rubber was developed in the structural laboratory of the Japan-Peru Center for Earthquake Engineering Research and disaster Mitigation. The low-cost seismic isolation prototype was tested under a free vibration and lateral reversal cyclic loading test, showing that the device has a good performance by dissipating the energy and shear strain deformation around 100% up to the failure. From the literature reviewed, a comparison of the stress-strain relationship is carried out and a modified stress-strain relationship to described the behavior of the developed device is proposed. Finally, comparing the response of a base isolated building and a fix building under an earthquake motion was performed. The results of the numerical simulations, show that the low-cost seismic isolation system proposed has a good performance by reducing the shear force induced to the building and the story drift of the isolated building.

*Keywords: performance assessment; low-cost; seismic isolation; recycled rubber; stress-strain relationship,*



## 1. Introduction

Seismic isolation system has been proved to be an efficient technology to protect buildings against earthquakes; a clear example of this occurred during the Great East Japan Earthquake in 2011 where many seismic isolated building did not suffer significant damages during the ground motion, moreover, buildings were kept operational post-disaster. [1][2]

As Peru is located in a high seismic hazard zone, it is necessary to protect essential buildings like hospitals, governmental buildings, etc., as it is required in the Seismic-Resistant Design Peruvian Standard, to ensure the life of its inhabitants, to keep the structure and non-structural elements without any damage, and that the building remains operational post-disaster.[3]

Seismic isolation system is expensive to afford, especially in developing countries; to protect buildings that are not categorized as essential buildings, such as dwellings, or other minor structures, it will be almost impossible to afford the use of this kind of system. For this reason, a prototype of isolator device with low cost of manufacture were developed, ABC for its acronym in Spanish (Aislador de Bajo Costo), using recycled rubber tire sheets. Three specimens were manufactured, and tested under a free vibration test and a lateral reversal loading test, under a constant axial load around 10tonf and a maximum shear strain around 100%. [4]

Based on a proposed modified Bouc-Wen hysteresis model [5], the aim of this research is to evaluate the performance of a base isolated system for a masonry dwelling, using the developed prototype ABC, through a time history analysis, considering the height of the masonry building up to 4 story and different soil conditions.

## 2. Outline of the Test and Test Result

### 2.1 Specimens

There specimens were manufactured (ABC-01, ABC-02 and ABC-03). The raw material used was recycled rubber tires, the rubber tire was cut into a square shape sheet of 20cm x 20cm and about 1.1cm of thickness, the internal wire mesh was kept as a contribution for the vertical stiffness of the isolator support, amount of wire-reinforcement is about 8.59% of the cross-section.

Rubber tire sheets was joined to each other using a vulcanization process, with a rubber layer of 3mm thickness made of recycled rubber tire powder in between rubber tire sheets; and in between the rubber tire sheet and the steel plate at both ends of the bearing. In total 4 rubber tire sheets was used, with a total height of the bearing of 6cm. the geometry of the specimen can be appreciated in Fig. 1



Fig. 1 – ABC specimen



## 2.2 Free Vibration Test

A free vibration test was conducted in order to determine the dynamic properties of the specimens, by applying an impulse and initial deformation to the specimen and recording the displacement and acceleration of the specimen. By processing the recorded data, it is possible to determine the natural vibration frequency, natural period, and inherent damping.

To carry out the free vibration test, different dead loads were applied on top of the isolators (see Fig. 2), then, a sequence of initial impulse and initial deformation was applied to the specimen. The measurement system to record the response of the specimen during the test was composed of accelerometers and laser displacement transducers at the bottom and the top of the specimen.



Fig. 2 – Free vibration test with different dead load applied

The displacement and acceleration response of the specimens was recorded as is shown in Fig. 3. The data was processed through filtering the noise. Using the processed data, a Fast Fourier Transform Analysis was performed; from the Fourier spectrums of the specimen, its fundamental period was calculated. Also, from the Weight vs Period graph shown in Fig. 4, is possible to calculate the initial stiffness of the specimen.

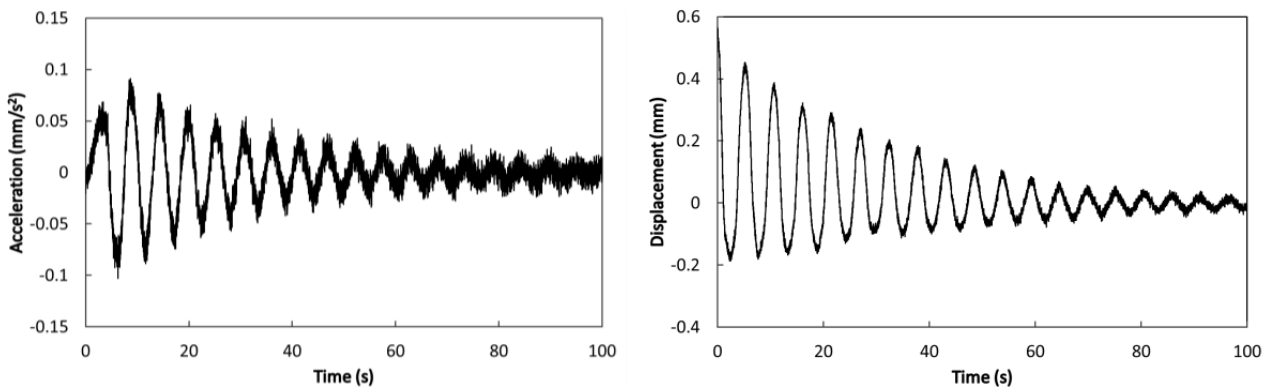


Fig. 3 – Free vibration test. Left: Acceleration response. Right: Displacement response

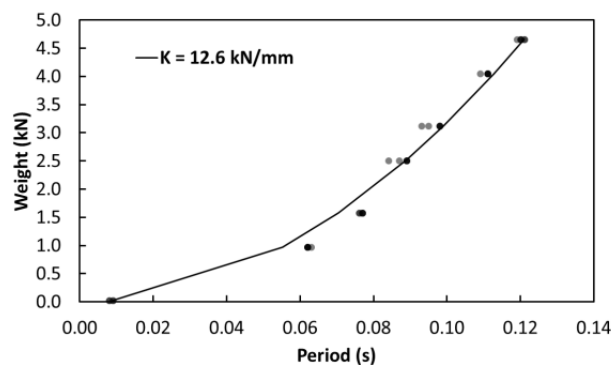


Fig. 4 – Weight vs Period of specimen ABC-02



### 2.3 Lateral Reversal Loading Test

To study the nonlinear response of the specimens against lateral reversal loading, three specimens were tested in a cyclic lateral reversal loading. To carry out the test, a constant axial load of about 100kN was applied on top of the specimen, which is the mean axial load obtained by the analysis of the target building, and a lateral displacement pattern with increasing levels of shear deformations up to the failure (see Table 1).

Table 1 – Displacement target and number of cycles

ABC-01		ABC-02		ABC-03	
Disp (mm)	# of Cycle	Disp (mm)	# of Cycle	Disp (mm)	# of Cycle
±4	2.5	±2	3	±2	3
±8	3.5	±3.5	3	±3.5	3
±13	4	±6.5	3	±6.5	3
±28	3	±9.5	3	±9.5	3
±42	3	±15	3	±15.5	3
±58	1	±30	3	±30.4	4
		±45.5	3	±45	3
		±61.2	1	±61.7	3
				±77.7	1

The setup of the loading frame and measuring system is shown in Fig. 5.

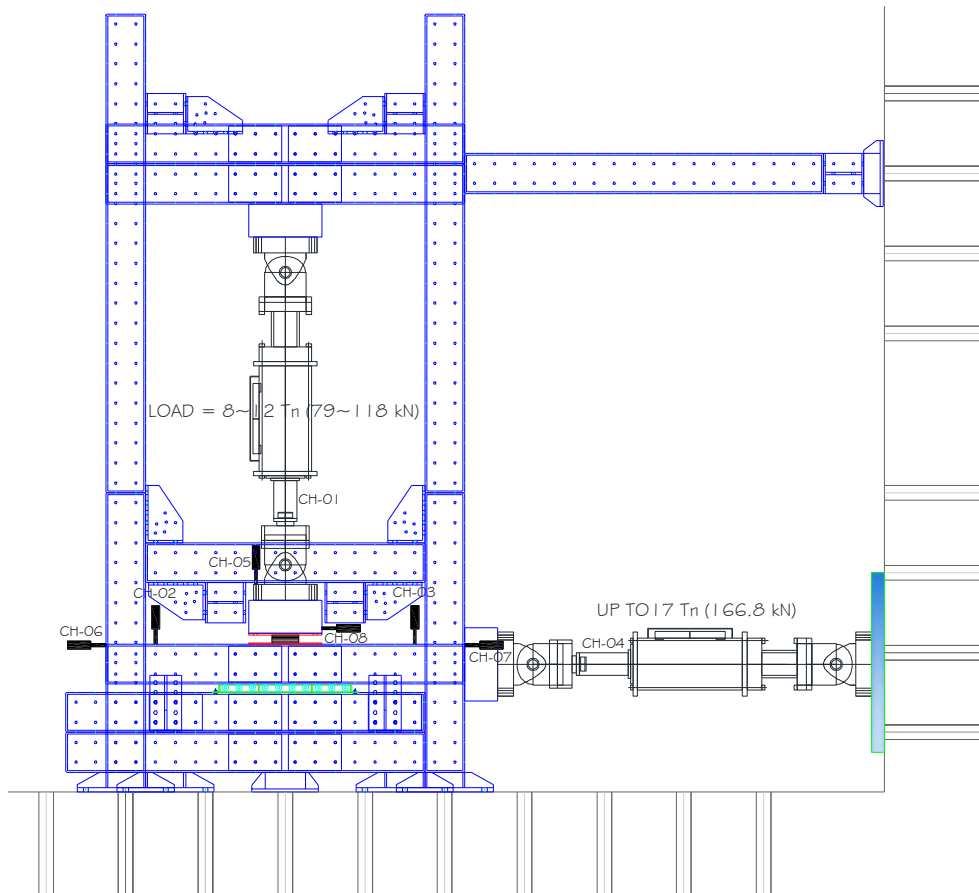


Fig. 5 – Setup of the loading frame and measuring system



For the load measurement, two load cells were used; meanwhile, the horizontal and vertical displacements of the top and bottom of the isolator were measured using displacement transducers, which distribution is shown in Fig. 5. The loading frame and specimen ABC-02 during the test is shown in Fig. 6.



Fig. 6 – Loading frame and specimen

As an example, after processing the experimental data recorded by filtering the noise, correcting the frictional force and deleting the pauses during the test; Fig. 7 shows the displacement pattern as well as the hysteresis curve of specimen ABC-02.

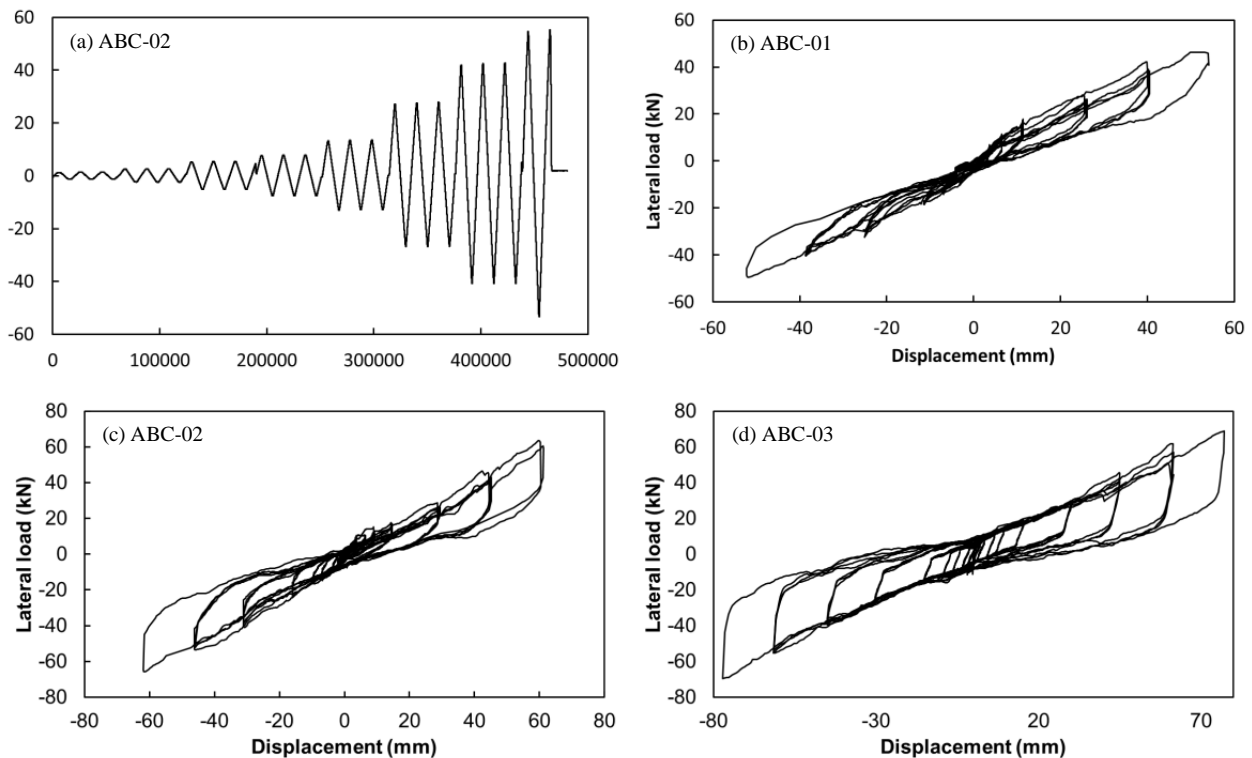


Fig. 7 – Displacement pattern (a) and hysteresis curve (b)(c)(d)

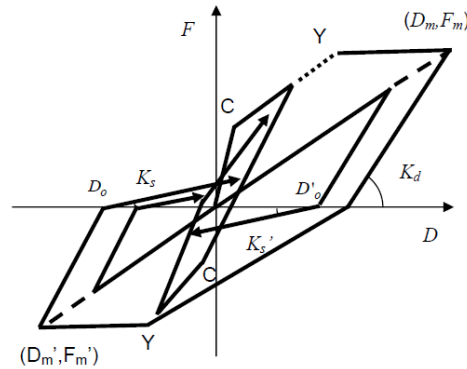


### 3. Review of the Stress-Strain Relationship Models

The essential hypothesis to model a base isolated building, is that the structure above the isolation level will remain elastic or very close to the elastic behavior, which in other words means that the upper-structure will not suffer significant damage. Takeda-slip model will be use to model the behavior of the upper-structure. On the other hand, the base isolated system will be modeled using a nonlinear hysteretic model based on Bouc-Wen model.

#### 3.1 Stress-strain relationship of the building structure

The upper-structure will be modeled by using Takeda-slip model. Eto and Takeda (1973) modified the Takeda model to incorporate a slip-type behavior at low stress level due to pull-out of longitudinal reinforcement from the anchorage zone. The skeleton curve is tri-linear with stiffness changes at cracking and yielding where the cracking and yielding levels can be different in positive and negative directions. The performance of the model is identical to the Takeda model before yielding. [11]



The reloading pinching stiffness  $K_s$  is defined by Eq. (1), the unloading stiffness for the same pinching loop  $K_d$  is defined by Eq. (2) and the slip stiffness  $K_p$  is defined by Eq. (3)

$$K_s = \frac{F_m}{D_m - D_o} \left| \frac{D_m}{D_y} \right|^{-\gamma} \quad (1)$$

$$K_d = \frac{F'_c + F_y}{D'_c - D_y} \left| \frac{D_m}{D_y} \right|^{-\alpha} \quad (2)$$

$$K_p = \eta \left( \frac{F_m}{D_m} \right)$$

Where  $D_o$  is the displacement at the end of the unloading (force equal to zero),  $D_m$  and  $F_m$  are the maximum deformation and force in the direction of loading,  $D_y$  and  $F_y$  are the yielding deformation and yielding force in the direction of loading and  $\gamma$  is the slip stiffness degradation factor (suggested to be equal to 0.5)

Where  $D'_c$  and  $F'_c$  are the deformation and resistance at the cracking point on the opposite side, is the displacement at the end of the unloading (resistance equal to zero),  $D_m$  and  $F_m$  are the maximum deformation and resistance,  $D_y$  is the yielding deformation and  $\gamma$  is the slip stiffness degradation factor (suggested to be equal to 0.5)



### 3.2 Stress-strain relationship of the seismic isolation system

The stress strain-relationship of the isolation system is based on the Bouc-Wen Model. The basic formula of Bouc-Wen model, described by Ikhrouane [6] and Saito [7] is shown in Eq.(3) and (4).

$$f = \alpha k_0 x + (1 - \alpha) k_0 z \quad (3)$$

$$\dot{z} = \frac{A\dot{x} - (\beta|\dot{x}||z|^{N-1}z + \gamma\dot{x}|z|^N)\nu}{\eta} \quad (4)$$

Where,  $\beta$ ,  $\gamma$  and  $N$  are parameters that control the shape of the hysteresis loop, while  $A$ ,  $\nu$  and  $\eta$  are variables that control the material degradation.

However, the original Bouc-Wen model does not fit well with the experimental data due to the lack to reproduce the pinching effect and the hardening effect at the end of the loop so, inspired on the Bouc-Wen Baber and Noori model [8] and using the properties of the Gauss bell, a modified Bouc-Wen model is proposed. This model is described by the Eq. (5), (6), (7) and (8). The described hysteretic model is controlled by 11 parameters:  $\alpha$ ,  $\beta$ ,  $\gamma$ ,  $\omega_n$ ,  $A$ ,  $n$ ,  $s_1$ ,  $\sigma_1$ ,  $d$ ,  $s_2$ ,  $\sigma_2$ . [4]

$$u_{(t)} = \ddot{x} + 2\xi\omega_n\dot{x} + \alpha\omega_n^2x + (1 - \alpha)\omega_n^2z \quad (5)$$

$$\dot{z} = A\dot{x}_1 - (\beta|\dot{x}||z|^{n-1}z + \gamma\dot{x}|z|^n) \quad (6)$$

$$\dot{x}_2 = \sqrt{\frac{2s_1}{\pi\sigma_1}} \dot{x} e^{-\frac{x^2}{2\sigma_1^2}} - \sqrt{\frac{2s_2}{\pi\sigma_2}} \dot{x} e^{-\frac{(x-d\text{sgn}(\dot{x}))^2}{2\sigma_2^2}} \quad (7)$$

$$x = x_1 + x_2 \quad (8)$$

From the experimental data of the ABC-03 specimen, a comparison between the original Bouc-Wen model and the modified Bouc-Wen model is shown in Fig. 8 and Fig. 9, where it can be observe the good match between the modified Bouc-Wen model with the experimental data with an error less than 10% in reference to the experimental dissipated energy of the specimen.

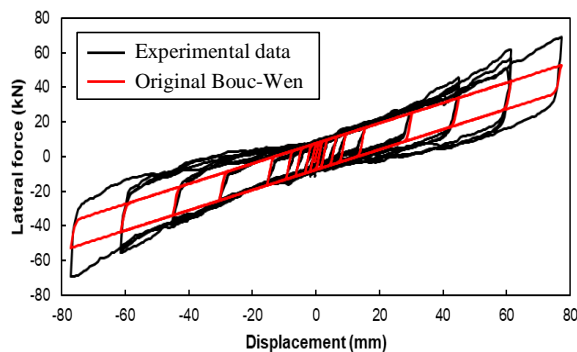


Fig. 8 – Original Bouc-Wen model

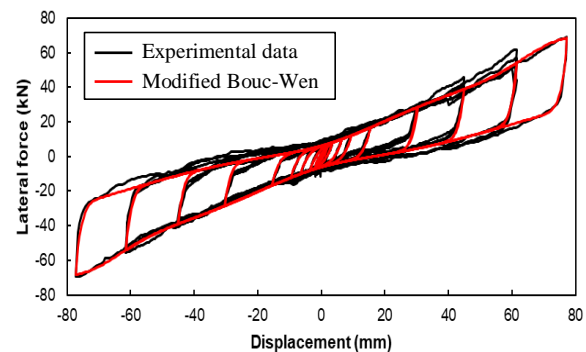


Fig. 9 – Modified Bouc-Wen model



## 4. Time History Analysis of the Target Building

### 4.1 Target Building

To perform a Time History Analysis, the target building considered is a masonry dwelling located in Lima city, and categorized as common building according to the Peruvian Standard E.030 Earthquake-Resistant Design [3]. Considering a typical floor plan for the building as is shown in Fig. 10, the target building was analyzed considering a different number of story.

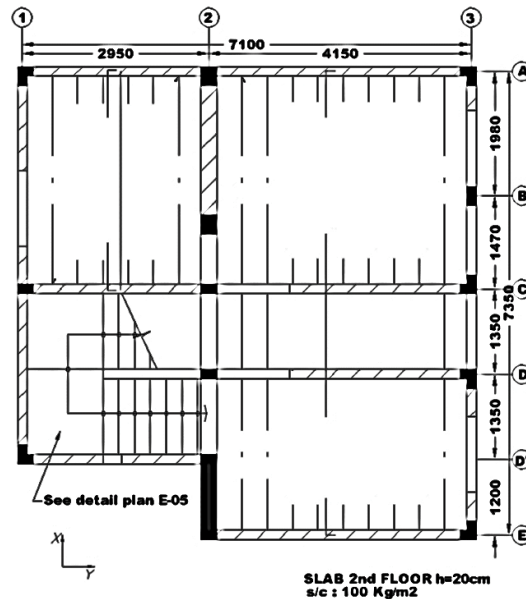


Fig. 10 – Floor plan of the masonry dwelling

### 4.2 Comparison of the fixed and base isolated building

Two models were analyzed, the first one consist of 2 story fixed base building and the second one is a 2 story base isolated building using 16 ABC-3 isolators due to the axial loads transmitted to the isolators oscillate between 100kN and 120kN. Considering soil type condition S1 and S2 according to the Earthquake-Resistant Standard E.030[3], Fig. 11 shows the comparison of the displacement response of a fixed base and a base isolated masonry dwelling, where a significant displacement reduction can be observed.

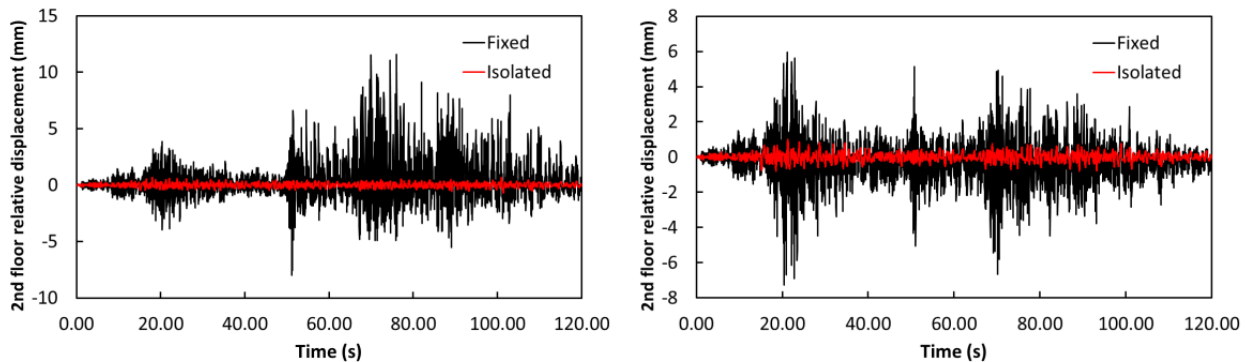


Fig. 11 – Displacement response of fixed and isolated building. Left: soil S1. Right: soil S2

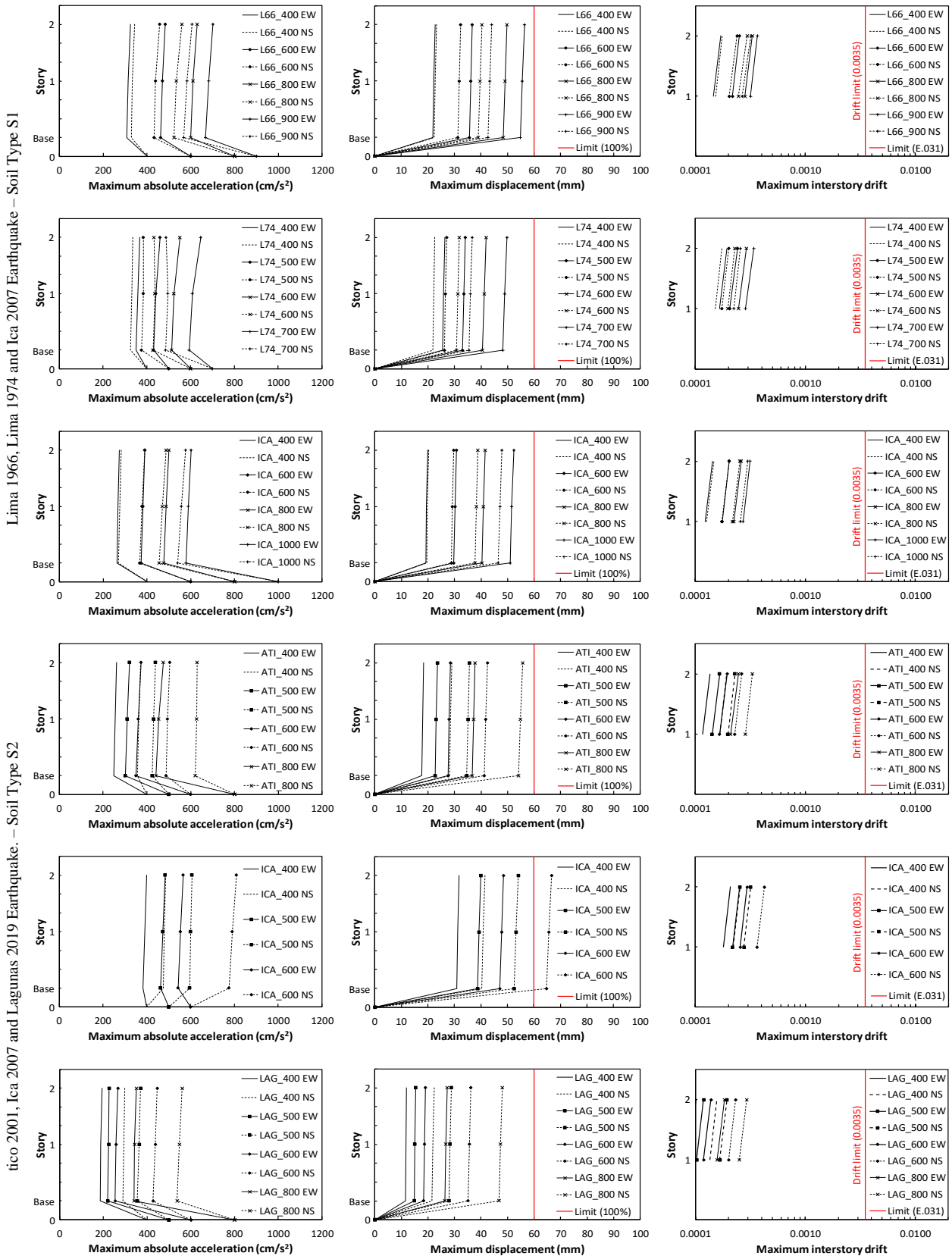


Fig. 12 – Earthquake response analysis of 2 story masonry dwelling

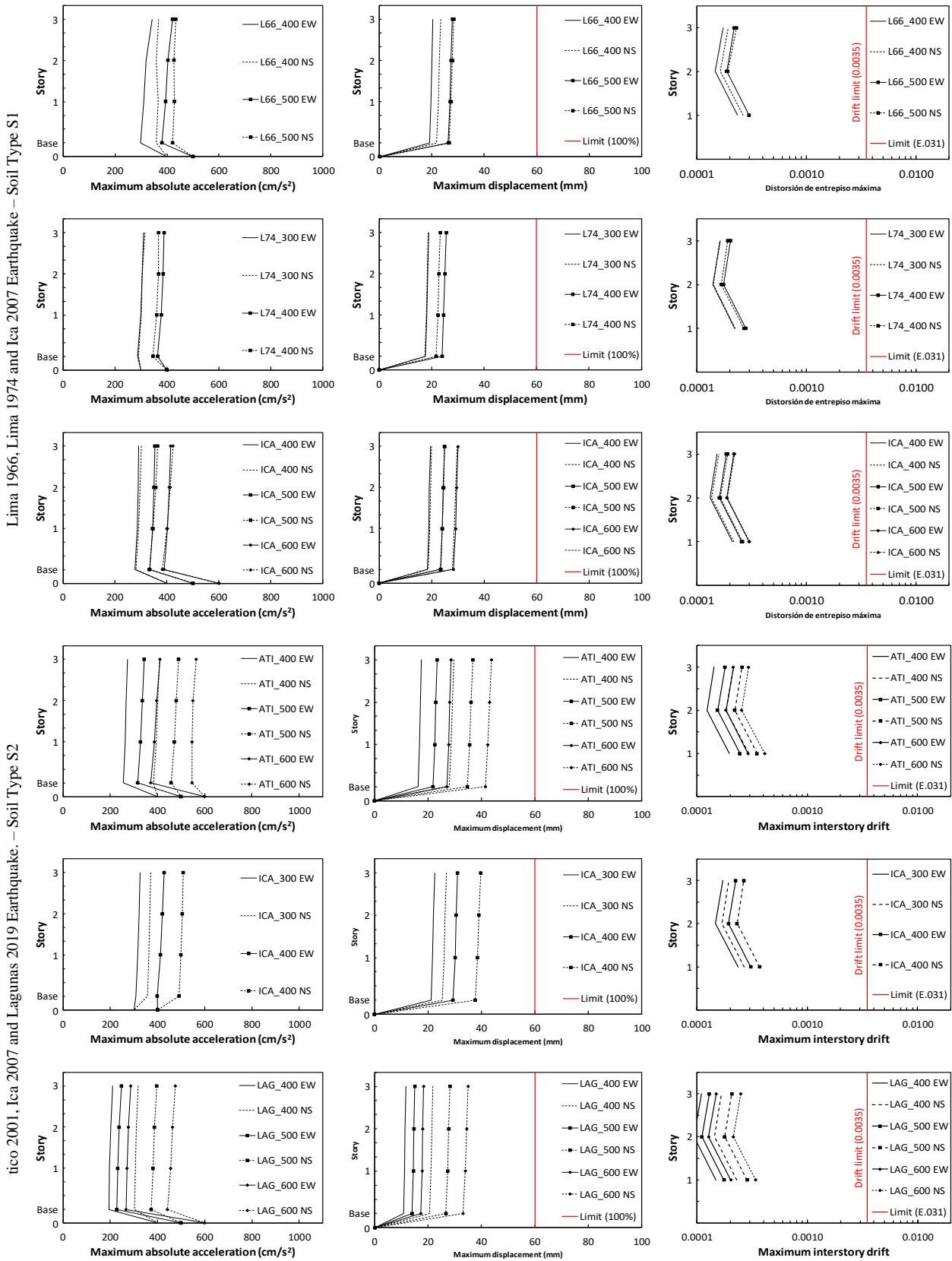


Fig. 13 – Earthquake response analysis of 3 story masonry dwelling

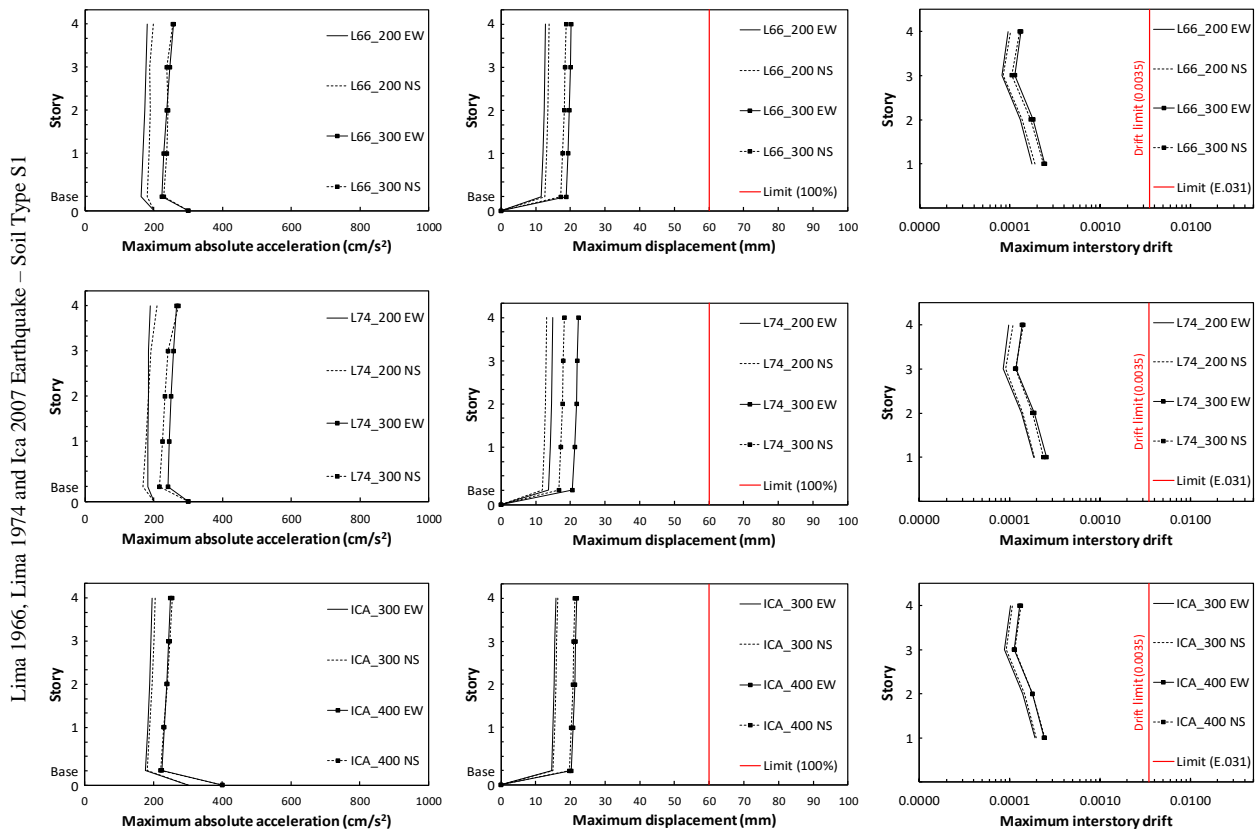


Fig. 14 – Earthquake response analysis of 4 story masonry dwelling

In addition to considering the soil condition, to evaluate the influence of the height of the building, the number of story will vary from 2 to 4, and a time history analysis will be carried out considering 5 historical Peruvian earthquakes (Lima 1966, Lima 1974, Atico 2001, Ica 2007 and Lagunas 2009). To conduct the simulations, earthquake records were scaled to a different values of PGA in order to assess the performance of the isolation system under different levels of accelerations.

From the experimental test, the specimens were taken up to a maximum shear strain deformation around 100%, equal to 60 mm, this limitation will be used as a boundary to control the performance of the models in terms of maximum displacement as is shown in Fig. 12, Fig. 13 and Fig. 14. On the other hand, taking into consideration the Peruvian Standard of Seismic Isolation E0.31 [9], base isolated buildings has an inter-story drift limitation equal to 0.0035; this value will be used to control the maximum inter-story drift of the upper-structure under different earthquakes records and peak ground accelerations.

From the earthquake response analysis of a masonry dwelling with different number of story, considering different soil conditions and under the action of different earthquake records scaled to different values of PGA, shown in Fig. 12, Fig. 13 and Fig. 14; base isolated building decouples the induced earthquake force to the upper-structure by reducing the maximum acceleration of the upper-structure and concentrating the displacement at the base isolation level, therefore, keeping lower displacements in the upper-structure. In terms of the inter-story drift of the upper-structure, the building is under the drift limitation mentioned above.

## 5. Conclusions

From the experimental results the specimens failed at around 100% of the rubber strain deformation of the specimen, therefore the maximum shear deformation considered for this study is 60 mm. From the numerical simulations, all the earthquake records were under this displacement limitation, except ICA\_600 NS that has a maximum displacement higher than 60 mm.



Considering the maximum inter-story drift equal to 0.0035, all the earthquake records were under this drift limitation, which means that the building has no significant damage in the upper-structure, and that the displacement is concentrated at the isolation level.

Proposed hysteresis model, gives a good approach of the experimental results, however the model has 11 parameters that controls the model, therefore it is necessary to improve the model to better characterize it by an adequate choosing of the parameters based on experimental information.

ABC specimens were considered to work in compression, but rocking effect were shown during the test, therefore the numerical analysis were considered up to a rocking tolerance were not tension force in the isolator is allowed.

## 6. Acknowledgements

The authors would like express their gratitude to the researchers and research assistant who contribute significantly during the experimental test as well as to the technicians of CISMID for their valuable support for the preparations of the tests.

## 7. Copyrights

17WCEE-IAEE 2020 reserves the copyright for the published proceedings. Authors will have the right to use content of the published paper in part or in full for their own work. Authors who use previously published data and illustrations must acknowledge the source in the figure captions.

## 8. References

- [1] Reyna R, Saito T (2012): Numerical simulation of base isolated buildings during the Great East Japan Earthquake and a proposal for a design procedure of base isolation system in Peru, *Bulletin of the International Institute of Seismology and Earthquake Engineering*, 47, 103-108.
- [2] Reyna R, Saito T, Zavala C, (2013). Numerical simulation of base isolated buildings during the Great East Japan Earthquake and a comparison of different hysteresis models, *Technical Paper, 13th World Conference on Seismic Isolation, Energy Dissipation and Active Vibration Control of Structures*, Sendai, Japan.
- [3] Ministry of Housing, Construction and Sanitation (2018): Technical Standard E.030 Earthquake-Resistant Design.
- [4] Reyna R, Muñoz A, Zavala C, Diaz M (2018): Prototype of low-cost seismic isolator using recycled tire sheets. Technical Paper No. 11323, *16th European Conference on Earthquake Engineering*, Thessaloniki, Greece.
- [5] Muñoz A, Diaz M, Reyna R (2019): Applicability study of a low cost seismic isolator prototype using recycled rubber. *TECNIA*, 29(2).
- [6] Ikhoulane F, Mañosa V, Rodellar J (2007): Dynamic properties of the hysteretic Bouc-Wen model, *Technical Paper, Systems & control letters*. 56, 197-205.
- [7] Saito T (2019): STERA3D Structural Earthquake Response Analysis 3D Technical Manual version 6.3. Toyohashi University of Technology, Japan.
- [8] Baber TT, Noori, MN (1985): Random vibration of degrading, pinching systems. *Journal of Engineering Mechanics*. 111(8), 1010-1026.
- [9] Ministry of Housing, Construction and Sanitation (2019): Technical Standard E.031 Seismic Isolation.
- [10] Eto H, Takeda Y (1973): Elasto Plastic Earthquake Response Analysis of Reinforced Concrete Frame Structure (in Japanese). Report, Annual Meeting, *Architectural Institute of Japan*. 1261-1262.
- [11] Otani S, (2002): Nonlinear Earthquake Response Analysis of Reinforced Concrete Buildings. Lecture Notes, Department of Architecture, Graduate School of Engineering, University of Toyo, Japan.